

MHD stagnation point flow and heat transfer in viscoelastic fluid with Cattaneo–Christov heat flux model

Y. Mehmood¹ · M. Sagheer¹ · S. Hussain¹ · M. Bilal¹

Received: 7 September 2016 / Accepted: 13 February 2017 / Published online: 23 February 2017
© The Natural Computing Applications Forum 2017

Abstract This article presents an analysis of stagnation point of coupled flow and heat transfer of an upper-convected Maxwell fluid over a stretching sheet along with magnetic effects and slip condition at the boundary. The recently proposed Cattaneo–Christov model is employed in the energy equation to investigate the effects of thermal relaxation time. Similarity transformations are adopted to convert the governing partial differential equations into ordinary differential equations. Numerical solution of the system of ODEs is achieved by shooting method together with Runge–Kutta method of order four. The effects of stretching ratio parameter ($0 \leq e \leq 0.5$), elasticity number ($0 \leq \beta \leq 1.5$), heat flux relaxation time ($0 \leq \gamma \leq 1.5$), magnetic parameter ($0 \leq M \leq 1.5$), slip coefficient ($1 \leq b \leq 4$) and Prandtl number ($0 \leq Pr \leq 1.5$) on velocity and temperature are investigated graphically and numerically. It is observed that temperature boosts up with an increase in thermal relaxation time.

Keywords Stagnation point · Magnetohydrodynamics · Cattaneo–Christov heat flux model · Upper-convected Maxwell fluid

List of symbols

a, c	Constants (1/time)
b	Slip coefficient
e	Stretching ratio parameter ($\frac{c}{a}$)
T_w	Wall temperature (K)
f'	Dimensionless velocity ($\frac{m}{s}$)

M	Magnetic parameter
\mathbf{V}	Velocity vector ($\frac{m}{s}$)
Pr	Prandtl number ($\frac{v}{\alpha}$)
α	Thermal diffusivity ($\frac{m^2}{s}$)
η	Similarity variable (m)
σ	Electrical conductivity ($\frac{S}{m}$)
λ_1	Relaxation time of the fluid (s)
σ_v	Tangential momentum accommodation
θ	Dimensionless temperature (K)
B_0	Magnetic field strength (T)
c_p	Specific heat ($\frac{J}{kgK}$)
T	Temperature of fluid (K)
T_∞	Ambient temperature (K)
(x, y)	Coordinate axis (m)
k	Thermal conductivity ($\frac{W}{mK}$)
\mathbf{q}	Heat flux ($\frac{J}{s}$)
(u, v)	Velocity components ($\frac{m}{s}$)
β	Elasticity number
ρ	Density of fluid ($\frac{kg}{m^3}$)
λ_0	Free path of molecular mean
λ_2	Relaxation time of heat flux (s)
ν	Kinematic viscosity ($\frac{m^2}{s}$)
γ	Thermal relaxation time (s)

1 Introduction

In nature, heat transfer in a fluid has a significant effect which happens due to difference in temperature within the same body or between two bodies. Many researchers have worth seeing contributions in this regard such as [1–8]. In various practical situations, Fourier’s model provides the basis to analyze the heat transfer phenomenon. But its

✉ Y. Mehmood
yasir7283@gmail.com; yasir.mehmood@cust.edu.pk

¹ Department of Mathematics, Faculty of Computing, Capital University of Science and Technology, Islamabad, Pakistan

major drawback was parabolic energy equation which yields that the initial disturbance can affect the whole system. To counter this shortcoming, Cattaneo [9] amalgamates the thermal relaxation time into the classical Fourier's law in order to get the hyperbolic energy equation. By introducing thermal relaxation time instead of diffusion in Fourier's law, heat transfer in the form of waves with finite speed is observed. In order to obtain invariant formulation of the material, Christov [10] modified the Cattaneo law by thermal relaxation time along with Oldroyd's upper-convected derivatives. The study of thermal convection in the Cattaneo–Christov model was carried by Straughan [11]. For the incompressible fluid, Tibullo and Zampoli [12] explained the uniqueness of Cattaneo–Christov heat flux model. Han et al. [13] studied the coupled flow and heat transfer in upper-convected Maxwell fluid over a stretching sheet by employing Cattaneo–Christov heat flux model. Khan et al. [14] investigated the upper-convected Maxwell fluid combined with heat transfer effects over an exponentially stretching surface by taking Cattaneo–Christov heat flux model.

The flow surrounded by a stagnation point has gained a considerable attention among several researchers during the past few decades. It has extensive applications at industrial level, e.g., nuclear reactors cooling all along emergency restrain, solar central receivers unprotected to wind currents, electronic devices cooling by fans and several hydrodynamic processes. Initially Hiemenz [15] proposed the concept of stagnation point flow. According to his theory, stagnation point flow describes the motion of fluid particles which are adjacent to the stagnation region of a solid surface for both fixed and moving bodies. Idea of Hiemenz was further extended by Homann [16] by considering the effect of stagnation point flow in three-dimensional geometry. Recently Turkyilmazoglu [5] investigated the stagnation point flow along with the slip effects on the MHD Jeffrey fluid and heat transfer over deformable surfaces.

Maxwell fluid has received a prominent consideration of researchers in recent era. The main advantage of Maxwell fluid is that it incorporates the relaxation time for the viscoelastic fluid in boundary layer flow. Choi et al. [17] investigated the flow of Maxwell fluid in a channel, in which, by increasing Deborah number, the viscoelasticity affects the velocity profiles in the same pattern as inertia in a Newtonian fluid with a fixed Reynolds number. Boundary layer flow of MHD upper-convected Maxwell fluid over a porous channel was analyzed by Abbas et al. [18], in which they considered the combined effects of viscoelasticity, inertia and applied magnetic field to yield an analytical solution. The impact of MHD and thermal radiation on Maxwell fluid over a stretching sheet was discussed by Aliakbar et al. [19]. According to their observation, an increase in the magnetic parameter and

elasticity number causes an enhancement in the heat transfer rate from the stretching sheet to the fluid. Mustafa [20] considered an upper-convected Maxwell fluid for rotating flow and heat transfer in the presence of Cattaneo–Christov heat flux model. Kumaria et al. [21] investigated the MHD mixed convection stagnation point flow of an upper-convected Maxwell fluid. They concluded that with the increase in the elasticity number, reduction in the surface heat transfer, surface velocity gradient and displacement thickness was experienced. Sadeghy et al. [22] examined the stagnation point flow of upper-convected Maxwell fluid, in which they negate the previously well-established prediction about the stagnation point flow of viscoelastic fluids, which states that the velocity inside the boundary layer may exceed from the outside layer. Hayat et al. [23] studied the stagnation point flow of an upper-convected Maxwell fluid for mass transfer. Effect on stagnation point flow of an upper-convected Maxwell fluid for heat transfer over a stretching sheet was analyzed by Hayat et al. [24]. Hayat et al. [25] discussed the stagnation point flow and heat flux in the Cattaneo–Christov model over a nonlinear stretching surface with variable thickness along with homogeneous–heterogeneous reactions in Maxwell fluid having variable thermal conductivity.

The main aspiration of the present study is to sort out the numerical solution of boundary layer stagnation point flow and heat transfer of viscoelastic fluid. Two models namely upper-convected Maxwell fluid model and Cattaneo–Christov heat flux model are considered for the formulation of momentum and energy equation. To obtain the numerical solution of the problem, similarity transformation and shooting method play a key role. However, these types of problems in a limiting case can be solved analytically. Turkyilmazoglu [6] proposed multiplicity of the analytical solution by considering the exponential and algebraic type solutions. Turkyilmazoglu [8] presented the some equivalences between the stretching plate problems over different configuration in two–three dimensions. According to his study, he proposed three different geometrical configurations which are mathematically equivalent to two-dimensional system. The influence of physical parameters on temperature and velocity profiles is investigated.

2 Mathematical model

Consider two-dimensional steady, laminar and incompressible stagnation point flow of a viscoelastic fluid over a semi-infinite plate coinciding with the plane $y = 0$. The plate is supposed to have a constant temperature T_w and the ambient fluid temperature T_∞ as shown in Fig. 1. Magnetic field of strength B_0 is applied normally to the direction of flow. Due to the consideration of small magnetic Reynolds number, the electric field is absent and induced magnetic field is neglected.

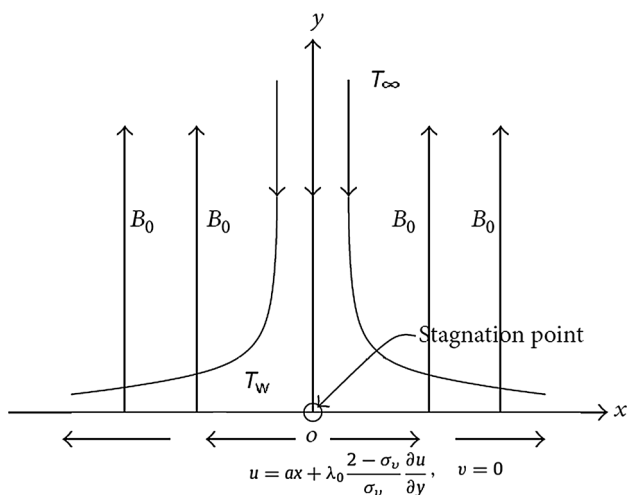


Fig. 1 Geometry of the model

Further first-order velocity slip condition is assumed at the wall. The heat flux model introduced by Cattaneo–Christov is taken into consideration. By using standard boundary layer approximations, the governing equations for the continuity, momentum and temperature flow are [5, 13] and [23]:

$$\frac{\partial u}{\partial x} + \frac{\partial v}{\partial y} = 0 \tag{1}$$

$$u \frac{\partial u}{\partial x} + \frac{\partial u}{\partial y} + \lambda_1 \left(u^2 \frac{\partial u^2}{\partial x^2} + v^2 \frac{\partial u^2}{\partial y^2} + 2uv \frac{\partial u^2}{\partial x \partial y} \right) = v \frac{\partial^2 u}{\partial y^2} + u_e \frac{du_e}{dx} + \frac{\sigma B_0^2}{\rho} \left(u_e - u - \lambda_1 v \frac{\partial u}{\partial y} \right) \tag{2}$$

$$\rho c_p \mathbf{V} \cdot \nabla T = -\nabla \cdot \mathbf{q} \tag{3}$$

The corresponding velocity slip boundary conditions [26] are:

$$\left. \begin{aligned} u &= ax + \lambda_0 \frac{2 - \sigma_v}{\sigma_v} \frac{\partial u}{\partial y}, \quad v = 0, \quad T = T_w \text{ at } y = 0, \\ u_e(x) &= cx, \quad T \rightarrow T_\infty \text{ as } y \rightarrow \infty. \end{aligned} \right\} \tag{4}$$

The heat flux \mathbf{q} satisfies the following relation:

$$\mathbf{q} + \lambda_2 \left[\frac{\partial \mathbf{q}}{\partial t} + \mathbf{V} \cdot \nabla \mathbf{q} - \mathbf{q} \cdot \nabla \mathbf{V} + (\nabla \cdot \mathbf{V}) \mathbf{q} \right] = -k \nabla T, \tag{5}$$

where $\mathbf{V} = (u, v)$ is the velocity vector of the Maxwell fluid. If we choose $\lambda_2 = 0$, Eq. (5) corresponds to Fourier’s law. Continuity equation for the incompressible fluid implies $\nabla \cdot \mathbf{V} = 0$, which when used in Eq. (5) yields the following:

$$\mathbf{q} + \lambda_2 \left[\frac{\partial \mathbf{q}}{\partial t} + \mathbf{V} \cdot \nabla \mathbf{q} - \mathbf{q} \cdot \nabla \mathbf{V} \right] = -k \nabla T, \tag{6}$$

Eliminating \mathbf{q} from Eqs. (3) and (6), we get:

$$u \frac{\partial T}{\partial x} + v \frac{\partial T}{\partial y} + \lambda_2 \left(\left(u \frac{\partial u}{\partial x} + v \frac{\partial u}{\partial y} \right) \frac{\partial T}{\partial x} + \left(u \frac{\partial v}{\partial x} + v \frac{\partial v}{\partial y} \right) \frac{\partial T}{\partial y} \right) + u^2 \frac{\partial^2 T}{\partial x^2} + v^2 \frac{\partial^2 T}{\partial y^2} + 2uv \frac{\partial^2 T}{\partial x \partial y} = \alpha \frac{\partial^2 T}{\partial y^2} \tag{7}$$

Introducing the following dimensionless variables:

$$\eta = \sqrt{\frac{a}{v}} y, \quad \psi = \sqrt{av} x f(\eta), \quad \theta(\eta) = \frac{T - T_\infty}{T_w - T_\infty} \tag{8}$$

After simplification we come forth with the following ordinary differential equations:

$$f''' + ff'' - f'^2 + \beta(2ff'f'' - f^2f''') + M(e - f' + \beta ff''') + e^2 = 0 \tag{9}$$

$$\frac{1}{Pr} \theta'' + f\theta' - \gamma(ff'\theta' + f^2\theta'') = 0. \tag{10}$$

The transformed boundary conditions of (4) are:

$$\left. \begin{aligned} f'(0) &= 1 + bf''(0), \quad f(0) = 0, \quad \theta(0) = 1, \quad f'(\infty) = e, \quad \theta(\infty) = 0. \end{aligned} \right\} \tag{11}$$

Different dimensionless parameters appearing in Eqs. (9)–(11) are defined as:

$$\begin{aligned} \beta &= \lambda_1 a, \quad \gamma = \lambda_2 a, \quad e = \frac{c}{a}, \quad M = \frac{\sigma B_0^2}{\alpha \rho}, \quad Pr = \frac{v}{\alpha} = \frac{\mu c_p}{k}, \\ b &= \lambda_0 \frac{2 - \sigma_v}{\sigma_v} \sqrt{\frac{a}{v}}. \end{aligned} \tag{12}$$

The skin friction coefficient C_f and local Nusselt number Nu are defined as:

$$C_f = \frac{\tau_w}{\rho(ax)^2}, \quad Nu = \frac{xq_w}{\alpha(T_w - T_\infty)}. \tag{13}$$

Here the wall shear stress τ_w and the heat flux q_w are defined as:

$$\tau_w = \mu(1 + \beta) \left(\frac{\partial u}{\partial y} \right)_{y=0}, \quad q_w = -\alpha \left(\frac{\partial T}{\partial y} \right)_{y=0}. \tag{14}$$

The dimensionless form of skin friction and Nusselt number is:

$$Re_x^{1/2} C_f = (1 + \beta) f''(0), \quad Re_x^{-1/2} Nu_x = -\theta'(0). \tag{15}$$

3 Numerical solution

The resulting nonlinear system of ordinary differential Eqs. (9) and (10) subject to the conditions (11) has been explored numerically through shooting method [27] for various values of the concerned parameters. On the basis of number of computational experiments, as there is no significant difference in the results after $\eta = 7$, we are considering $[0, 7]$ as the domain of the problem instead of $[0, \infty)$. We have chosen the following nomenclature for converting the boundary value problem to the initial value problem consisting of five first-order ordinary differential equations.

$$f = y_1, f' = y_2, f'' = y_3, \theta = y_4, \theta' = y_5 \tag{16}$$

The coupled nonlinear momentum and heat equations are transformed into the following system of five first-order differential equations along with initial conditions.

$$\left. \begin{aligned} y_1' &= y_2, & y_1(0) &= 0 \\ y_2' &= y_3, & y_2(0) &= 1 + by_3(0) \\ y_3' &= \frac{[-y_1y_3(1 + 2\beta y_2) + y_2^2 - M(e - y_2 + \beta y_1y_3) - e^2]}{1 - \beta y_1^2}, & y_3(0) &= s \\ y_4' &= y_5, & y_4(0) &= 1 \\ y_5' &= \frac{\text{Pr}y_1y_5(\gamma y_2 - 1)}{1 - \gamma \text{Pr}y_1^2}, & y_5(0) &= t \end{aligned} \right\} \tag{17}$$

We apply the Runge–Kutta method of order four to solve the above initial value problem. To refine the values of s and t , we apply the Newton’s method until we meet the following criteria.

$$\max\{|y_2(7) - e|, |y_4(7) - 0|\} < \varepsilon, \tag{18}$$

where $\varepsilon > 0$ is a small positive real number. All the numerical results in this paper are achieved with $\varepsilon = 10^{-5}$.

4 Results and discussion

In this article, we utilized the upper-convected Maxwell fluid with Cattaneo–Christov heat flux model to explore the boundary layer flow and heat transfer above a stretching plate with velocity slip boundary condition. Although we have achieved almost the same numerical results for different quantities of interest by two different techniques, for more gratification, we feel a need to validate our MATLAB code by implementation on some published work of the similar nature. For this purpose, we reproduced the numerical values of skin friction for the models investigated by Sadeghy et al. [22] and Abel et al. [28]. An impressively

convincing agreement of our results with those of Sadeghy et al. and Abel et al. is given in Table 1. Table 2 presents the values of skin friction and Nusselt number for different emerging parameters. Temperature gradient at the sheet shows increasing behavior for the stretching ratio parameter, Prandtl number and thermal relaxation time, while it depicts inverse behavior for elasticity number, slip coefficient and magnetic parameter. Similarly skin friction seems to have an increasing trend for elasticity number and magnetic parameter and decreasing for slip coefficient and stretching ratio parameter.

A relation between upper-convected Maxwell and Newtonian fluid models is set up by an elastic term. Heat transfer and fluid flow are influenced by elastic force. Figures 2 and 3 depict the influence of elasticity number β on velocity and temperature profile. Viscoelastic fluid turns into Newtonian fluid by ignoring the effects of elastic force β . With an increase in the value of β , the elastic forces strengthen up. By enhancement in β , velocity profile shows decreasing and temperature distribution possesses an increasing flow patterns in the viscous fluid. It is because of the fact that an increase in the elasticity number leads to the stronger viscous force which opposes the fluid motion and as a result the velocity displays decreasing pattern. Figures 4 and 5 illustrate the influence of magnetic parameter M on velocity and temperature boundary layer flow. Magnetic field is applied along normal to the fluid flow. It is observed that magnetic field opposes the fluid motion and enhances the temperature distribution. Figures 6 and 7 present the slip effects on velocity and temperature profile. Velocity shows the decreasing behavior for increment in the value of b and converse for the temperature profile. Figures 8 and 9 show the effect of stretching ratio e over velocity and temperature distribution. With the increase in the stretching ratio, we experienced an increase in the velocity profile and decrement in the thermal boundary layer. When $e < 1$, the stretching sheet velocity axis is greater than the velocity of the far

Table 1 Comparison of numerical values of $-f''(0)$ with [15] and [21] for $M = e = \gamma = b = 0$ and $\text{Pr} = 1$

β	$-f''(0)$		
	Sadeghy [15]	Abel [21]	Present
0.0	1.0000	0.999962	1.0001725
0.2	1.0549	1.051948	1.0519731
0.4	1.10084	1.101850	1.1019446
0.6	1.0015016	1.150163	1.1501584
0.8	1.19872	1.196692	1.1967224
1.2	–	1.285257	1.2853239
1.6	–	1.368641	1.3673413
2.0	–	1.447617	1.4463152

Table 2 Numerical values of $-(1 + \beta)f''(0)$ and $-\theta'(0)$ for different parameters

e	Pr	γ	β	b	M	Shooting		bvp4c	
						$-(1 + \beta)f''(0)$	$-\theta'(0)$	$-(1 + \beta)f''(0)$	$-\theta'(0)$
0.1	1	0.1	0.1	0.1	0.05	0.968554	0.575354	0.968554	0.575354
						0.915324	0.602832	0.915324	0.602832
						0.845289	0.630777	0.845289	0.630777
	0.5					0.968554	0.368480	0.968554	0.368480
		1.5				0.968554	0.744492	0.968554	0.744492
		2.5				0.968554	1.017927	0.968554	1.017927
	1	0.2				0.968554	0.583098	0.968554	0.583098
		0.4				0.968554	0.599482	0.968554	0.599482
		0.5				0.968554	0.608089	0.968554	0.608089
			0.2			1.077807	0.600289	1.077807	0.600288
			0.4			1.305184	0.585631	1.305184	0.585631
			0.8			1.790399	0.561494	1.790399	0.561494
				0.2		1.554512	0.540975	1.554512	0.540975
				0.5		1.134616	0.498868	1.134161	0.498868
				0.9		0.848754	0.463693	0.848754	0.463693
					0.5	0.933687	0.424693	0.933687	0.424693
					1	1.002469	0.395878	1.002469	0.395878
					1.5	1.054939	0.375867	1.054939	0.375867

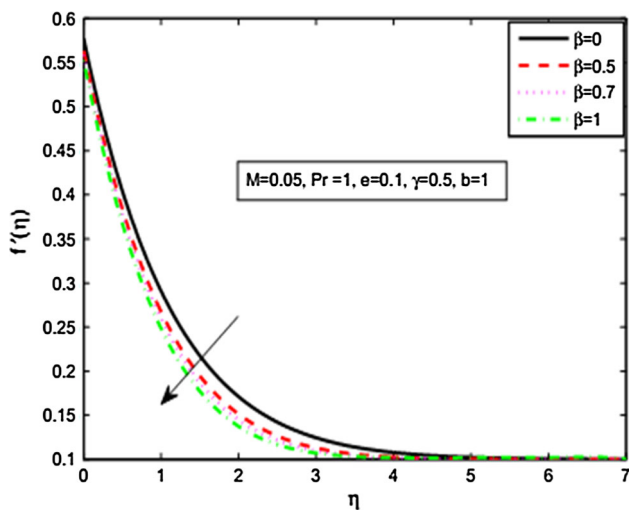


Fig. 2 Influence of β on $f'(\eta)$

stream cx . Figure 10 presents the effects of thermal relaxation time γ on temperature profile. Temperature profile shows decreasing behavior for enhancement in the thermal relaxation time. Fourier’s Law can be deduced from the present model by applying $\gamma = 0$. It is noticed that the temperature in Cattaneo–Christov heat flux model is smaller than the Fourier’s model. Figure 11 shows that with the increase in Prandtl number Pr the temperature boundary layer becomes thinner, because Prandtl number has an inverse relationship with the thermal diffusivity. Figure 12 represents the relationship of Nusselt number in accordance with the Prandtl number Pr and thermal relaxation time γ ,

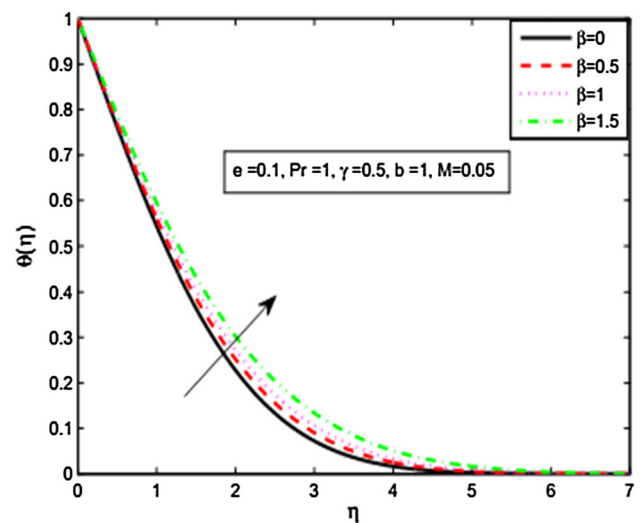


Fig. 3 Influence of β on $\theta(\eta)$

with the increase in the Prandtl number Pr thermal relaxation time γ depicts an increasing behavior. All the calculations are performed in hp(i5) machine with 4 GB RAM, and it takes 1.561 s to plot a single graph.

5 Concluding remarks

The present model addresses the magnetic effects in stagnation point flow on upper-convected Maxwell fluid along with the Cattaneo–Christov heat flux model. To solve the

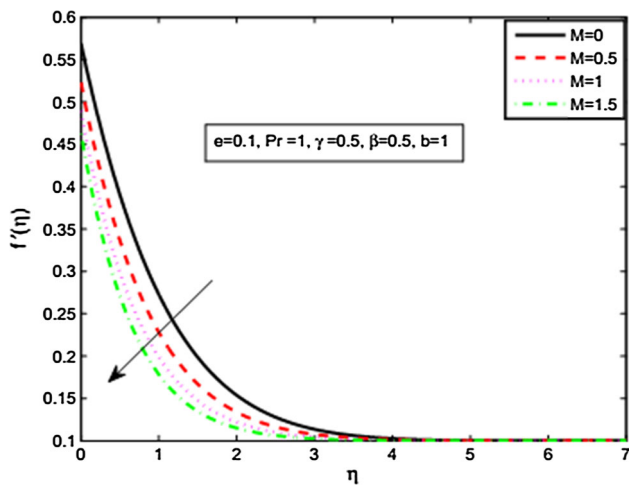


Fig. 4 Impact of M on $f'(\eta)$

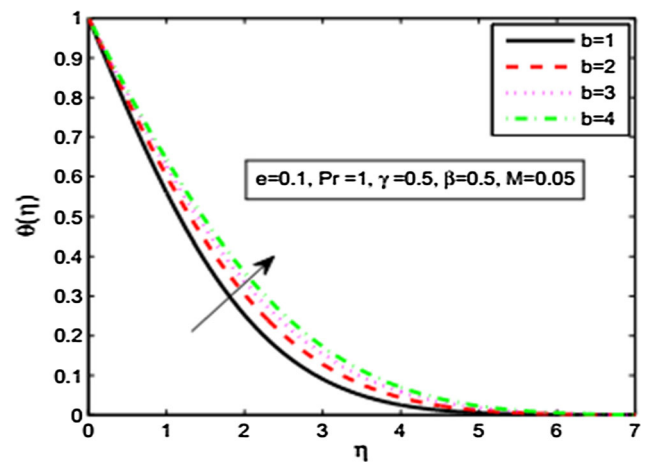


Fig. 7 Influence of b on $\theta(\eta)$

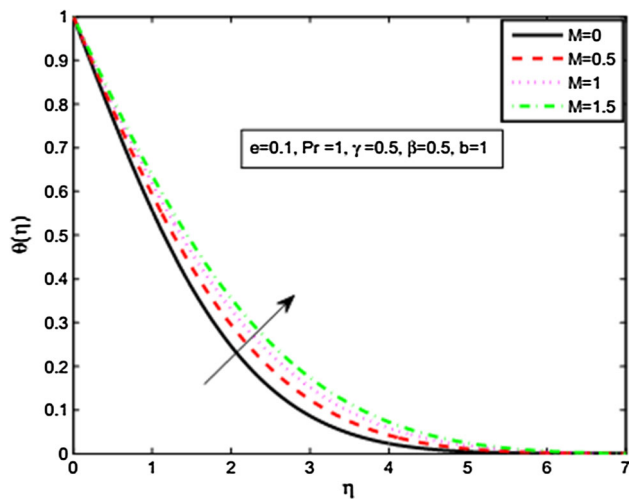


Fig. 5 Influence of M on $\theta(\eta)$

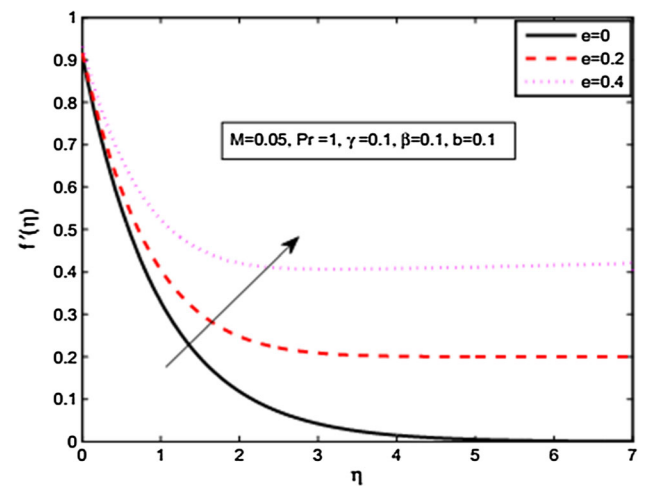


Fig. 8 Effect of e on $f'(\eta)$

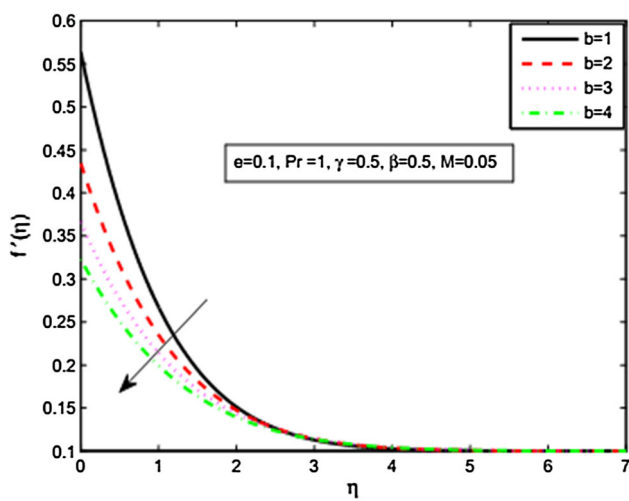


Fig. 6 Impact of b on $f'(\eta)$

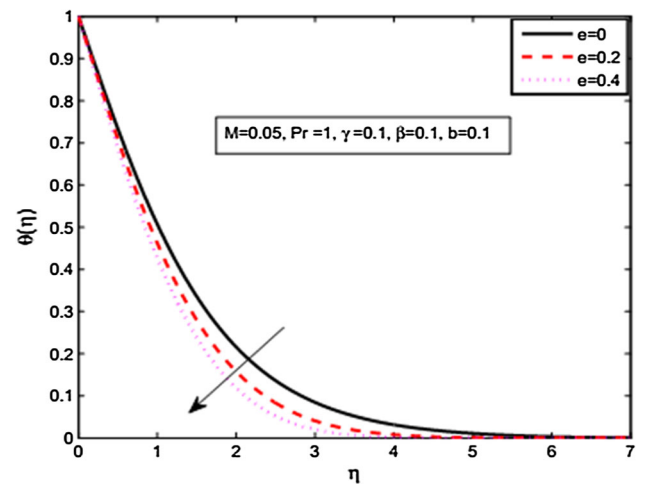


Fig. 9 Effect of e on $\theta(\eta)$

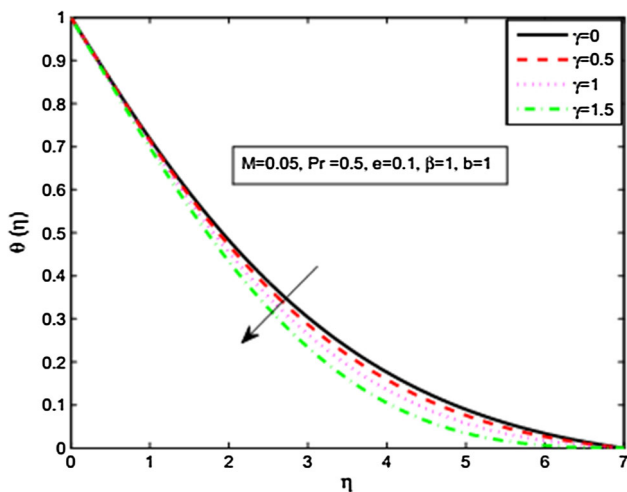


Fig. 10 Effect of γ on $\theta(\eta)$

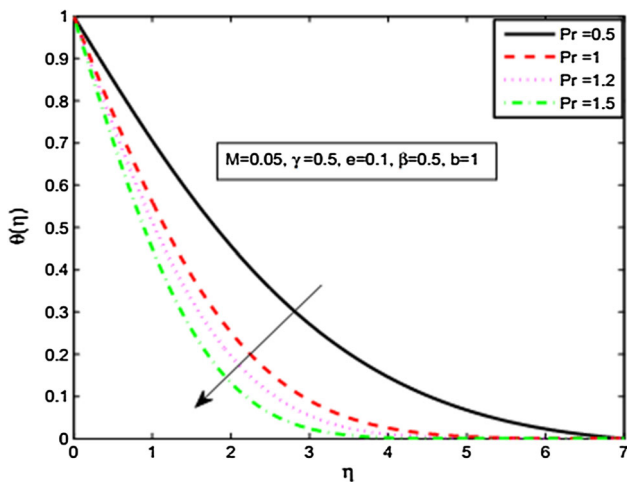


Fig. 11 Effect of Pr on $\theta(\eta)$

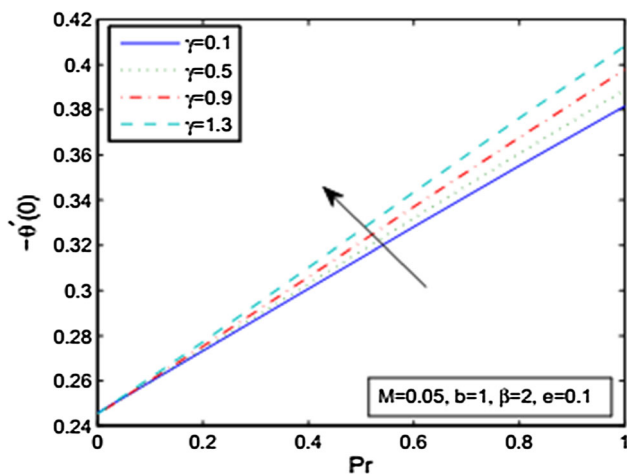


Fig. 12 Influence of Pr and γ on $Nu_x Re_x^{-1/2}$

system of coupled ordinary differential equations, we adopted shooting method. To strengthen the results, we also employed MATLAB built-in function bvp4c. The main observations are summarized as follows:

- By increasing the magnetic field intensity, velocity profile exhibits decreasing pattern and opposite behavior is seen in thermal boundary layer.
- Increase in the elasticity number and slip coefficients causes the decrease in velocity phenomenon and opposite behavior is observed in temperature profile.
- Enhancement in the stretching ratio parameter results in decrease in wall shear stress and an increment in Nusselt number.
- By increasing the thermal relaxation time, temperature raises up.

Compliance with ethical standards

Conflict of interest Authors have no conflict of interest for this publication.

References

1. Rashidi MM, Erfani E (2012) Analytical method for solving steady MHD convective and slip flow due to a rotating disk with viscous dissipation and ohmic heating. *Eng Comput* 29:562–579
2. Ab olbashari MH, Freido onimehr N, Nazari F, Rashidi MM (2014) Entropy analysis for an unsteady MHD flow past a stretching permeable surface in nano-fluid. *Powder Technol* 267:256–267
3. Rashidi MM, Ali M, Freidoonimehr N, Rostami B, Hossain MA (2014) Mixed convective heat transfer for MHD viscoelastic fluid flow over a porous wedge with thermal radiation. *Mech Eng Adv*. doi:10.1155/2014/735939
4. Freidoonimehr N, Rashidi MM, Mahmud S (2015) Unsteady MHD free convective flow past a permeable stretching vertical surface in a nano-fluid. *Int J Ther Sci* 87:136–145
5. Turkyilmazoglu M (2016) Magnetic field and slip effects on the flow and heat transfer of stagnation point Jeffrey fluid over deformable surfaces. *Int J Heat Mass Transf* 71:549–556
6. Turkyilmazoglu M (2015) An analytical treatment for the exact solutions of MHD flow and heat over two-three dimensional deforming bodies. *Int J Heat Mass Transf* 90:781–789
7. Turkyilmazoglu M (2012) Multiple analytic solutions of heat and mass transfer of magnetohydrodynamic slip flow for two types of viscoelastic fluids over a stretching surface. *J Heat Transf* 134:071701–1–071701–9
8. Turkyilmazoglu M (2016) Equivalences and correspondences between the deforming body induced flow and heat in two-three dimensions. *Phys Fluids* 28:043102–1–043102–10
9. Cattaneo C (1948) Sulla conduzione del calore. *Atti Semin Mat Fis Univ Modena Reggio Emilia* 3:83–101
10. Christov CI (2009) On frame indifferent formulation of the Maxwell–Cattaneo model of finite speed heat conduction. *Mech Res Commun* 36:481–486
11. Straughan B (2010) Thermal convection with the Cattaneo–Christov model. *Int J Heat Mass Transf* 53:95–98

12. Tibullo V, Zampoli V (2011) A uniqueness result for the Cattaneo–Christov heat conduction model applied to incompressible fluids. *Mech Res Commun* 38:77–99
13. Han S, Zheng L, Li C, Zhang X (2014) Coupled flow and heat transfer in viscoelastic fluid with Cattaneo–Christov heat flux model. *Appl Math Lett* 38:87–93
14. Khan JA, Mustafa M, Hayat T, Alsaedi A (2015) Numerical study of Cattaneo–Christov heat flux model for viscoelastic flow due to an exponentially stretching surface. *PLoS ONE* 10(9):e0137363
15. Hie menz K (1911) Die Grenzschicht an einem in den gleichförmigen flüssigkeitsstrom eingetauchten geraden Kreiszyylinder. *Ding Polytech J* 5:321–326
16. Homann F (1936) Die einfluss grsse zahigkeit bei der strömung um der zylinder und um die kugel. *J Appl Math Mech* 16:153–164
17. Choi JJ, Rusak Z, Tichy JA (1999) Maxwell fluid suction flow in a channel. *Non-Newtonian Fluid Mech* 85:165–187
18. Abbas Z, Sajid M, Hayat T (2006) MHD boundary-layer flow of an upper-convected Maxwell fluid in a porous channel. *Theor Comput Fluid Dyn* 20:229–238
19. Aliakbar V, Pahlavan AA, Sadeghy K (2009) The influence of thermal radiation on MHD flow of Maxwellian fluids above stretching sheets. *Commun Nonlinear Sci Numer Simul* 14:779–794
20. Mustafa M (2015) Cattaneo–Christov heat flux model for rotating flow and heat transfer of upper convected Maxwell fluid. *AIP Adv* 5:047109
21. Kumaria M, Nath G (2009) Steady mixed convection stagnation-point flow of upper convected Maxwell fluids with magnetic field. *Int J Non-Linear Mech* 44:1048–1055
22. Sadeghy K, Hajibeygib H, Taghavia SM (2006) Stagnation-point flow of upper-convected Maxwell fluids. *Int J Non-Linear Mech* 41:1242–1247
23. Hayat T, Awais M, Qasim M, Hendi AA (2011) Effects of mass transfer on the stagnation point flow of an upper-convected Maxwell (UCM) fluid. *Int J Heat Mass Transf* 54:3777–3782
24. Hayat T, Mustafa M, Shehzad SA, Obaidat S (2012) Melting heat transfer in the stagnation-point flow of an upper-convected Maxwell (UCM) fluid past a stretching sheet. *Int J Numer Meth Fluids* 68:233–243
25. Hayat T, Khan MI, Farooq M, Yasmeen T, Alsaedi A (2016) Stagnation point flow with Cattaneo–Christov heat flux and homogeneous-heterogeneous reactions. *J Mol Liq* 220:49–55
26. Sui J, Zheng L, Zhang X (2016) Boundary layer heat and mass transfer with Cattaneo Christov double-diffusion in upper-convected Maxwell fluid past a stretching sheet with slip velocity. *Int J Ther Sci* 104:461468
27. Na TY (1979) *Computational methods in engineering boundary value problems*. Academic Press, London
28. Abel MS, Tawade JV, Nandeppanavar MM (2012) MHD flow and heat transfer for the upper-convected Maxwell fluid over a stretching sheet. *Meccanica* 47:385393